

Center-Shift Circular Transformation Cavity

Jinhang Cho, Inbo Kim, and Sunghwan Rim

Digital Technology Research Center, Kyungpook National University, Daegu 41566, Republic of Korea

Jung-Wan Ryu

Center for Theoretical Physics of Complex Systems,
Institute for Basic Science (IBS), Daejeon 34126, Republic of Korea

Muhan Choi*

Digital Technology Research Center, Kyungpook National University, Daegu 41566, Republic of Korea

We analyzed the characteristics of conformal whispering gallery modes according to pure spatial refractive index variation without boundary deformation in two-dimensional center-shift circular transformation cavity designed in an alternative scheme without using resizable parameter. Through this, we confirmed that the isotropic emission of whispering gallery mode in the circular cavity with homogeneous refractive index is transformed into the bi-directional emission of conformal whispering gallery mode as the degree of center-shift increased. Also, using a newly defined purity factor that quantitatively measures the modulus of distortion, it was verified that the internal wave property of the whispering gallery mode maintained almost intact in the conformal whispering gallery mode.

PACS numbers: xx.xx

I. INTRODUCTION

Transformation cavities (TCs) are recently proposed optical dielectric cavities with the gradient refractive index (GRIN) designed based on transformation optics [1]. The optical dielectric cavities, especially the microcavities, have been intensively studied over the last two decades due to the applicability as the next generation of ultra-small high quality resonators used in integrated optical circuits and sensors [2–4]. One type of resonances with very long lifetime in the dielectric cavities, namely whispering gallery mode (WGM), is an important topic which has the largest portion of studying it. The WGMs are generated by trapping the waves inside the cavities by total internal reflection (TIR) phenomenon caused by the difference between the interior and exterior refractive indices (RIs) at the cavity boundary. The ideal WGMs in a circular dielectric cavity promise the highest quality-factor (Q -factor), but its isotropic emission characteristics due to the perfect rotational symmetry limit the applicability. In order to overcome this problem, many researches have been carried out to deform the cavity shape, but it also causes degradation of Q -factor and cumbersome phenomena such as the wave chaos [5–8] and the mode coupling effects [9–15]. TCs offer a powerful way to overcome these problems and its feasibility is also presented already [1]. So-called, the conformal whispering gallery modes (cWGMs) generated in the TCs have directional emission with minimal Q -factor spoiling. The TCs can be designed through various conformal mappings or the composite functions of multiple conformal mappings. Also, even if conformal mapping is singular or

non-existent, the quasi-conformal mapping method can be used to numerical access any possible shape [16].

Typically, the deformation effect in the homogeneous cavities is taken by the distortion of the geometrical boundary shape, which affects to the characteristics of the resonances, such as the changes in wavelength, Q -factor, wave patterns, and mode coupling effects. The variations of the boundary curvature ray-dynamically causes the unsatisfaction for the critical angle on the incident beam, which directly leads distortion of the WGMs which are formed by TIR mechanism. However, the distinction for the deformation effect is ambiguous in the case of TCs designed by basis of circular cavity. In the construction process of the TCs, the boundary deformation is firstly contained in the refractive index profile to perfectly cancel out by the conformal transformation for whole space, and finally, the residual effect formed by the gap between the conformal transformation and the artificial setting, which forces the exterior refractive index to 1, is survived in only the relative refractive index at the boundary interface [1]. It can be clearly understood through the description in RV space [17]. There are no changes in curvature, but changes in the relative refractive index at the boundary interface. The spatial refractive index variation results in a change in the critical angle at the boundary and then affects cWGM formation. The blending effects, combined with the condition to satisfy TIR, the composition of various conformal mappings, and the wave properties depending on the system openness or the wavelength regime [18–20], make more difficult and complicated to stipulate the mode characteristics according to the system parameters. Center-shift (C-S) circular TC is a special case that produces only the effects of purely spatial refractive index variation formed by the coordinate shift for center, which completely excludes the geometrical boundary deforma-

* mhchoi@ee.knu.ac.kr

tion effect. Moreover, it has manufacturing advantages because its original shape is retained regardless of the C-S degree. As a groundwork on the research for various TCs using the C-S conformal mapping, which can be used as an element of composite functions to achieve a realistic refractive index profile or to break axis symmetry, we investigated the cWGM characteristics for the C-S circular TCs in this study.

This paper is organized as follows. We briefly review the C-S conformal mapping and the conventional method for designing TCs using resizable parameter to support cWGMs in Sec. II. An alternative scheme to configure the TCs without resizable parameter and the C-S circular TC constructed through this scheme is introduced in Sec. III. In Sec. IV, the characteristics of cWGMs in C-S circular TC is numerically investigated and the purity factor for measuring the efficiency of cWGM is newly defined and discussed. Finally we give a summary in Sec. V.

II. CENTER-SHIFT CONFORMAL MAPPING AND CONVENTIONAL METHOD TO DESIGN TRANSFORMATION CAVITY

The C-S conformal mapping to give the effect of moving the center of a circle can be performed with the subgroup of Möbius transformation to complex ζ -space from complex η -space. The subgroup of Möbius transformations that map the unit circle to the C-S unit circle represented as following complex form,

$$\zeta = \frac{\eta + \delta}{1 + \delta^* \eta}, \quad |\delta| < 1,$$

where $\eta = u + iv$ and $\zeta = x + iy$ are spatial variables describing the complex planes, and δ is a complex value parameter for C-S degree on (u, v) coordinates. Considering the rotational symmetry of the circle, the mapping can be simplified by treating only the shift on the x -axis ($\delta \in \mathbb{R}$) as follows:

$$\zeta = f(\eta) = \frac{\eta + \delta}{1 + \delta \eta}, \quad |\delta| < 1. \quad (1)$$

By the application of the above conformal mapping, concentric circles in η -space are transformed into C-S circles of which the rotational symmetry is broken in ζ -space as shown in Fig. 1. For reference, the inverse conformal mapping from ζ -space to η -space is expressed as follows:

$$\eta = g(\zeta) = \frac{\zeta - \delta}{1 - \delta \zeta}, \quad |\delta| < 1. \quad (2)$$

Next, we look at the TCs which is previously proposed in [1]. Considering the translational symmetry along the z -axis in a infinite cylindrical dielectric cavity, the Maxwell equations can be reduced to effective 2-dimensional scalar wave equation. Resonances in

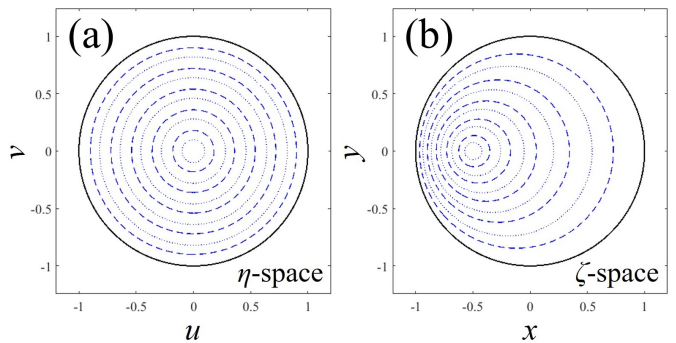


Figure 1. Conceptual diagrams for C-S conformal mapping from (a) η -space to (b) ζ -space using the subgroup of Möbius transformation.

a TC satisfying the outgoing-wave boundary condition, $\psi(\mathbf{r}) \sim h(\phi, k)e^{ikr}/\sqrt{r}$ for $r \rightarrow \infty$, where position vector $\mathbf{r} = (x, y) = (r \cos \phi, r \sin \phi)$, k is the vacuum wavenumber, and $h(\phi, k)$ is the far-field angular distribution of the emission, are obtained as the solutions of following wave equation,

$$[\nabla^2 + n^2(\mathbf{r})k^2] \psi(\mathbf{r}) = 0,$$

with the refractive index $n(\mathbf{r})$ given by

$$n(\mathbf{r}) = \begin{cases} n_0 \left| \frac{d\zeta}{d\eta} \right|^{-1}, & \text{(interior)} \\ 1, & \text{(exterior)} \end{cases}. \quad (3)$$

For the transverse magnetic (TM) polarization, the wave function $\psi(\mathbf{r})$ represents E_z , the z component of electric field, and both the wave function $\psi(\mathbf{r})$ and its normal derivative $\partial_v \psi(\mathbf{r})$ are continuous across the cavity boundary. For the transverse electric (TE) polarization, the wave function $\psi(\mathbf{r})$ represents H_z , the z component of magnetic field, and both $\psi(\mathbf{r})$ and $n(\mathbf{r})^{-2} \partial_v \psi$ are continuous across the cavity boundary. By the outgoing-wave boundary condition, the resonances, which have discrete complex wavenumbers k_r with negative imaginary parts, exponentially decay in time. The frequency and the lifetime of a resonance are given by $\omega = c\text{Re}[k_r]$ and $\tau = -1/2c\text{Im}[k_r]$ where c is light speed in vacuum, respectively. The quality factor of a resonance is defined as $Q = 2\pi\tau/T = -\text{Re}[k_r]/2\text{Im}[k_r]$ where the oscillation period of light wave is $T = 2\pi/\omega$.

To describe the conventional method for constructing TCs supporting cWGMs through the resizable parameter β , four spaces are usually considered: original virtual (OV), wholly transformed (WT), transformed physical (TP), and reciprocal virtual (RV) spaces. First, we consider a circular cavity with a homogeneous refractive index n_0 and a unit radius R_0 in η -space, and call this space OV space. The homogeneous unit circular cavity in the OV space is conformally transformed to a cavity with inhomogeneous interior and exterior refractive index

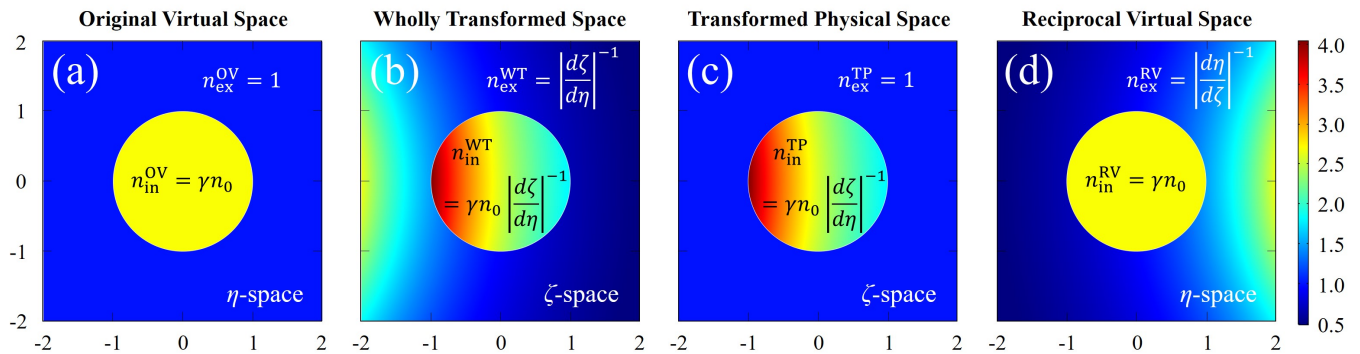


Figure 2. Refractive index profiles in (a) original virtual, (b) wholly transformed, (c) transformed physical, and (d) reciprocal virtual spaces. These pictures were drawn in center-shift circular transformation cavity without resizable parameter at $n_0 = 1.8$, $|\delta| = 0.2$, and $\gamma = \gamma_{\min}$.

profiles in ζ -space through a entire spatial mapping multiplied by β , such as a resizable C-S conformal mapping,

$$\zeta = \beta f(\eta) = \beta \frac{\eta + \delta}{1 + \delta\eta}, \quad |\delta| < 1.$$

We name this transformed space WT space. The two cavities in OV and WT spaces are mathematically equivalent and the relative refractive index at the boundary interface in WT space remains homogeneous. Next, we force the exterior GRIN profile in WT space to 1 considering the realistic physical situation then, finally, we can obtain a C-S circular TC in TP space. In TP space, the relative refractive index at the boundary interface is not homogeneous. The heterogeneity of the relative refractive index acts as an important factor in forming the resonance characteristics which differ from in circular cavity, and the reason can be easily predicted through the RV space which is mathematically equivalent to the TP space. The RV space can be defined by inversely transforming the entire refractive index profile in TP space. In order to obtain cWGMs in the conventional TCs, a specific value β_{\max} or lower is finally applied to β such that the minimum value of the internal refractive index profile is at least n_0 as a condition that allows the wave near the cavity boundary cause the TIR ray-dynamically through the process of reducing the cavity size. Therefore, $|d\zeta/d\eta|^{-1}$ which forms a inhomogeneous refractive index profile of TCs, is a function of β , so not only cavity size but refractive index profile changes according to the change of β .

III. CENTER-SHIFT CIRCULAR TRANSFORMATION CAVITY WITHOUT RESIZABLE PARAMETER

Here, we propose a new TC design scheme that maintains the dimensionless coordinates [2] in physical space by eliminating the size-scaling by conformal mapping.

We first consider a homogeneous circular cavity in OV space (η -space) with the unit radius R_0 and the invariant reference refractive index n_0 multiplied by an index-proportion parameter γ and conformally transform the cavity to WT space (ζ -space) by the mapping equation without β , Eq. (1). Then, forcing the exterior refractive index to 1 yields the TC in TP space. As a result, the interior and exterior refractive index in the TP space is as follows:

$$n(\mathbf{r}) = \begin{cases} n_{\text{in}}^{\text{TP}} = \gamma n_0 \left| \frac{d\zeta}{d\eta} \right|^{-1}, & (\text{interior}) \\ n_{\text{ex}}^{\text{TP}} = 1, & (\text{exterior}) \end{cases}. \quad (4)$$

Additionally, through the inverse transformation from ζ -space to η -space, the interior and exterior refractive index in RV space can be obtained as follows:

$$\tilde{n}(\tilde{\mathbf{r}}) = \begin{cases} n_{\text{in}}^{\text{RV}} = \gamma n_0, & (\text{interior}) \\ n_{\text{ex}}^{\text{RV}} = \left| \frac{d\eta}{d\zeta} \right|^{-1}, & (\text{exterior}) \end{cases}$$

where position vector $\tilde{\mathbf{r}} = (u, v)$. We shortly call the newly constructed TC to γ -type TC and, for clarity, we refer to the conventional TC as the β -type TC. γ -type TC can satisfy the TIR condition by increasing the interior refractive index in OV space independently of the profile-generating factor, $|d\zeta/d\eta|^{-1}$ of Eq. (4), without reducing the cavity size. This is the most noticeable difference from the β -type TC, in which decreasing β to satisfy the TIR condition reduces the cavity size and simultaneously increases the profile-generating factor of Eq. (3) as a whole. To help understand, we have drawn conceptual diagrams of four spaces using in the C-S circular γ -type TC in Fig. 2.

β -type and γ -type are perfectly identical systems in the viewpoint of physics and the differences between them are summarized in Table I. k_r in γ -type is the dimensionless resonant wavenumber and multiplying k_r by

$n_{\text{in}}^{\text{OV}}$ changed by γ gives the internal dimensionless resonant wavenumber, $\chi \equiv n_{\text{in}}^{\text{OV}} k_r = \gamma n_0 k_r$. The free-space wavenumber in β -type is obtained by dividing k_r in γ -type by β . One can properly select and use at convenience among the two types. γ -type can be more advantageous in terms of theoretical and numerical study such as analyzing the changes of resonance distribution in a given wavelength region, adjusting the target frequency of the resonance to be observed, tracing a specific resonance to finding the optimizing conditions, or reobtaining the refractive index profile for designing on real fabrication.

	β -type TC	γ -type TC
conformal transformation	$\zeta = \beta f(\eta)$	$\zeta = f(\eta)$
refractive index in OV space	$n_{\text{in}}^{\text{OV}} = n_0$	$n_{\text{in}}^{\text{OV}} = \gamma n_0$
radius of cavity in TP space	$\beta R_0 = \beta$	$R_0 = 1$
refractive index in TP space	$n_{\text{in}}^{\text{TP}} = n(\zeta, \beta)$	$n_{\text{in}}^{\text{TP}} = \gamma n(\zeta)$

Table I. Differences between β -type and γ -type TCs

By the C-S conformal mapping Eq. (1), the circular cavity with homogeneous interior refractive index $n_{\text{in}}^{\text{OV}} = \gamma n_0$ in OV space is transformed to the γ -type C-S circular TC with the following inhomogeneous interior refractive index profile in the TP space.

$$n_{\text{in}}^{\text{TP}}(\zeta) = \gamma n_0 \left| \frac{d\zeta}{d\eta} \right|^{-1} = \gamma n_0 \left| \frac{(1 - \delta\zeta)^2}{(\delta^2 - 1)} \right|^{-1}, \quad |\delta| < 1,$$

Also, we can derive the profiles of interior and exterior refractive index for γ -type TC in the RV space through the inverse conformal mapping Eq. (2) as follows:

$$n_{\text{in}}^{\text{RV}} = n_{\text{in}}^{\text{OV}} = \gamma n_0,$$

$$n_{\text{ex}}^{\text{RV}}(\eta) = \left| \frac{d\eta}{d\zeta} \right|^{-1} = \left| \frac{(1 - \delta^2)}{(1 + \delta\eta)^2} \right|, \quad |\delta| < 1.$$

To obtain cWGMs formed by TIR, the condition is required that the minimum value of the interior refractive index profile is at least greater than n_0 and we define γ satisfying this condition as γ_{min} . In the case of γ -type C-S circular TC, $n_{\text{in}}^{\text{TP}}$ has the minimum value at $\eta = -\delta/|\delta|$, thus γ_{min} is given as follows:

$$\gamma_{\text{min}} \equiv \gamma = \frac{1 + |\delta|}{1 - |\delta|}, \quad |\delta| < 1.$$

IV. NUMERICAL RESULTS

A. cWGMs in γ -type Center-Shift Circular Transformation Cavity

Using the γ -type C-S circular TC presented above, we investigate the characteristic changes of a specific

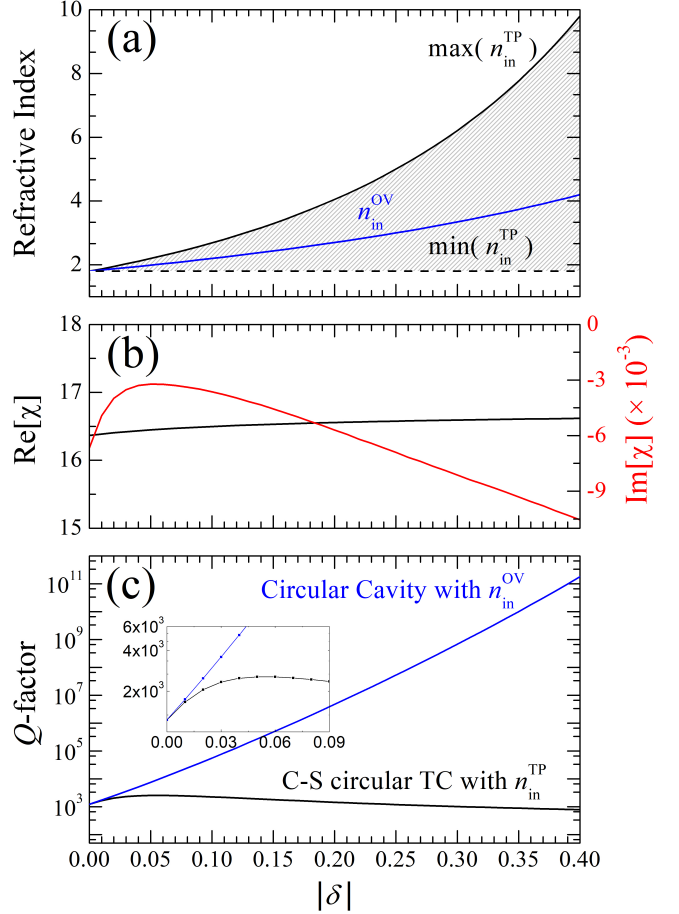


Figure 3. Changes of (a) refractive indices, (b) internal dimensionless wavenumber, and (c) Q -factors for M(13,1) according to the center-shift parameters $|\delta|$ in the γ -type C-S circular TC with $n_0 = 1.8$ and $\gamma = \gamma_{\text{min}}$. Black solid and black dashed lines in (a) are the maximum and the minimum values of refractive index profile $n_{\text{in}}^{\text{TP}}$, respectively. Blue solid line in (a) is $n_{\text{in}}^{\text{OV}}$ that varies with $|\delta|$. Black and red lines in (b) are the real and the imaginary parts of the internal dimensionless wavenumber, respectively. Black and blue lines in (c) are Q -factors in the γ -type C-S circular TC with $n_{\text{in}}^{\text{TP}}$ and the circular cavity with $n_{\text{in}}^{\text{OV}}$, respectively. Inset of (c) is an enlargement of $|\delta|$ from 0 to 0.09.

cWGM, M(13,1) for TM polarization by changing in the range of $0 \leq |\delta| \leq 0.4$ under the fixed conditions of reference refractive index $n_0 = 1.8$ and index-proportion parameter $\gamma = \gamma_{\text{min}}$. In this paper, we assign cWGMs to M(m , l) as a combination of mode indices corresponding to the angular momentum index m and the radial nodal number l in the homogeneous circular cavity. According to the change of $|\delta|$, the interior refractive index in OV space and the maximum and minimum value of interior refractive index profile in TP spaces are changed as shown in Fig. 3 (a). As $|\delta|$ increases, the maximum value of refractive index profile $n_{\text{in}}^{\text{TP}}$ gradually widens the overall variation of the index profile with n_0 as the baseline. At the same time, as the index profile widens, $n_{\text{in}}^{\text{OV}}$

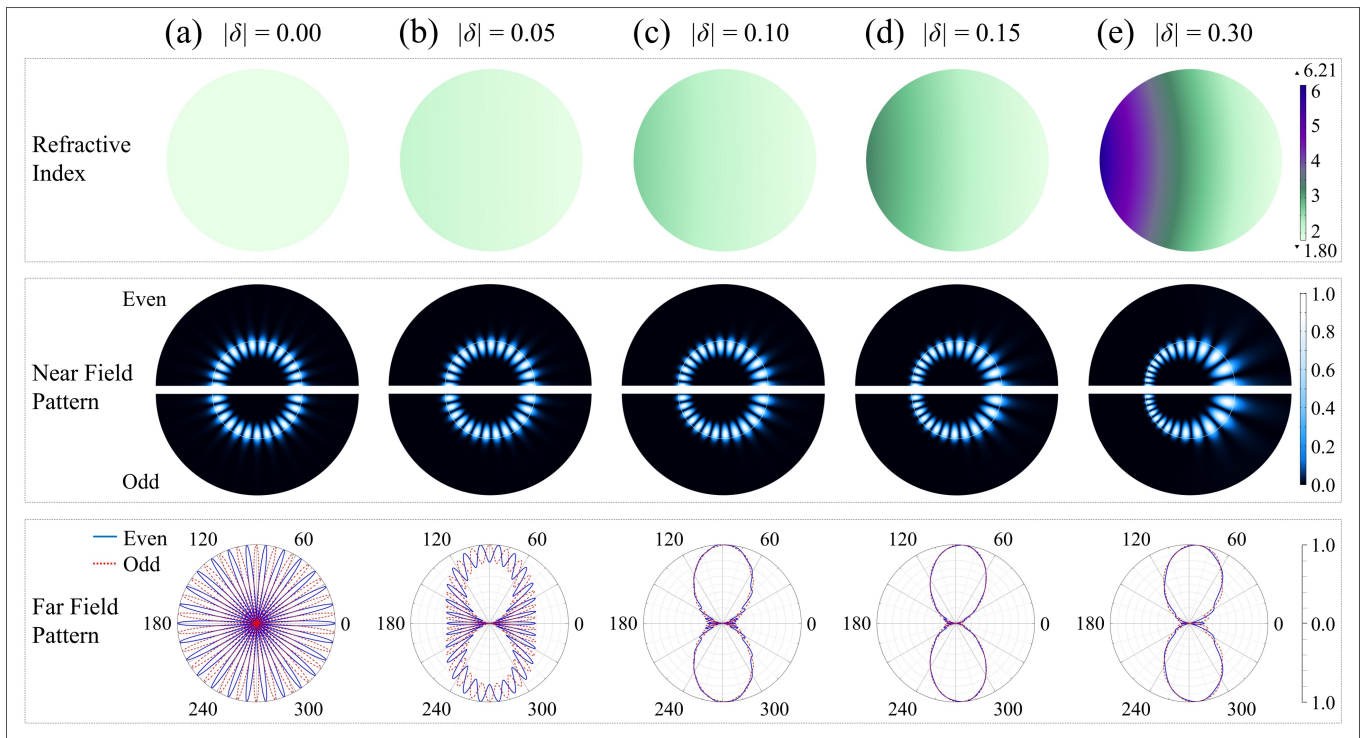


Figure 4. Refractive index profile and near field and far field intensity patterns for the mode pair of M(13,1) at the shifting parameter (a) $|\delta| = 0$, (b) 0.05, (c) 0.10, (d) 0.15, and (e) 0.30 in the γ -type C-S circular TC with $n_0 = 1.8$ and $\gamma = \gamma_{\min}$. The refractive index of outside cavity set to air. In each step, up-side (down-side) of near field pattern and blue solid (red dashed) line in far-field pattern are the even-parity (odd-parity) mode.

also increases to satisfy the TIR condition.

The internal dimensionless wavenumbers χ and Q -factors for the mode pair of M(13,1) are changed as shown in Fig. 3 (b) and (c), respectively. In the homogeneous circular cavity case with $|\delta| = 0$, all resonances except for the case with $m = 0$ are in doubly degenerate states due to the rotational symmetry. Each degenerate pair is nearly degenerate under the condition of $|\delta| > 0$ and each nearly degenerate pair can be divided into even- and odd-parity modes due to the mirror symmetry for the x -axis. Nevertheless, in the range we show, the wavelenth values for the cWGM pair appear to overlap almost one with no significant deviation. In terms of the RV space shown in Fig. 2 (d)), it means that the cWGM pair is very little affected by the pure change in relative refractive index at the boundary interface caused by $|\delta|$ in our range.

As shown in Fig. 3 (b), $\text{Re}[\chi]$ associated with the internal wavelength of the mode pair of M(13,1) does not change significantly with the varying in $|\delta|$, on the other hand, $\text{Im}[\chi]$ grows larger than that in the homogeneous case and then decreases from a certain threshold (in our case, about $|\delta| = 0.05$) as $|\delta|$ increases. It is directly reflected in the Q -factor in Fig. 3 (c). The temporary rise of Q -factor, which is typical aspect of cWGMs in TC satisfying the TIR condition [1, 21], is caused by the overall increasement in the refractive index profile of TC due to the TIR condition, and the increment of $n_{\text{in}}^{\text{OV}}$ in the γ -

type TC well explains why such behavior occurs as shown in the inset of Fig. 3 (c).

For the case of $|\delta| \neq 0$, the relative refractive index at the boundary interface and the interior refractive index profile exhibit a dipole distribution similar to the case of the limaçon TC [1]. Considering the emitting mechanism described through the Husimi function [17], cWGMs in the C-S circular TC can be predicted to have a similar mode properties. We show the stepwise change of refractive index profile and near- and far-field intensity patterns for a even-odd mode pair of M(13,1) at $|\delta| = 0, 0.05, 0.10, 0.15$, and 0.30 in Fig. 4. As $|\delta|$ increases, the dipole distribution of the refractive index becomes more pronounced due to the increase in the variation width of the index profile, while the near field intensity pattern at all steps maintains a cWGM morphology confined well along the boundary.

In Ref. [17, 21], it has already discussed that the emission of cWGMs satisfying the TIR condition is tunneled out as an evanescent wave in the region where the refractive index is relatively low and, as the deformation parameter increases, the nearly flat intensity band structure on the Husimi function for cWGMs is almost unchanged, while the shape of the critical line is further bent by the variation of the relative refractive index at the boundary interface. Such non-constant critical angle creates a unique light emission mechanism which the light tunnels

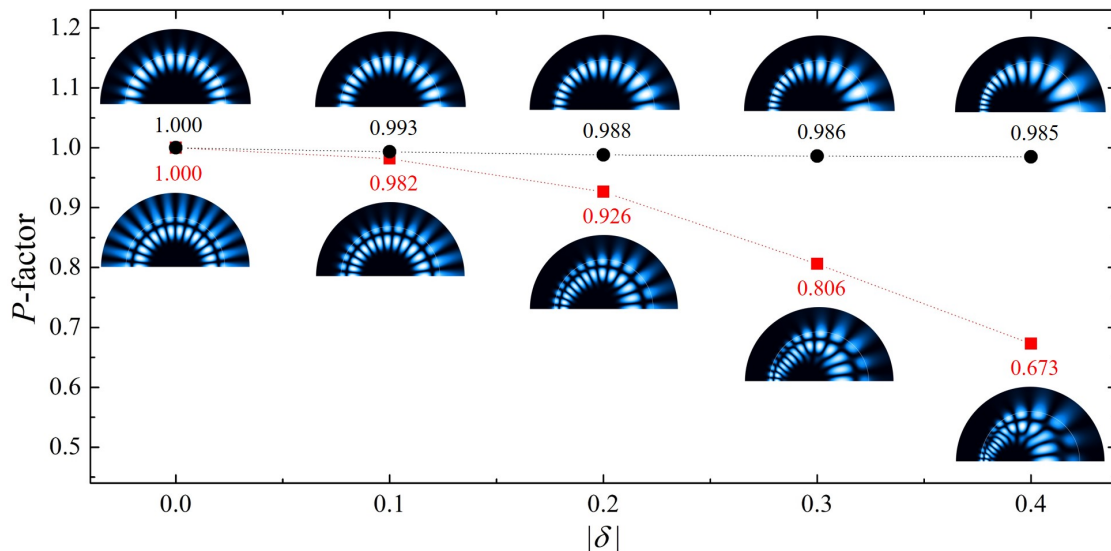


Figure 5. The change of P -factors for even-parity modes of (a) $M(13,1)$ and (b) $M(13,2)$ according to $|\delta|$ in γ -type C-S circular TC with $n_0 = 1.8$ and $\gamma = \gamma_{\min}$. The data pickup domain for P -factors is set to $r_{\text{RV}} = 0.8$ and the intensity of the near field patterns is normalized linear scale.

out at regions where the band structure is relatively close to the critical angle. i.e., where the relative refractive index at the boundary interface is relatively low.

In the TCs with a dipole distributed refractive index profile, the critical line approaches the band structure only in one place, which creates a single point emitting mechanism, and their external waves form bi-directional emission if they have an axis symmetry. We can confirm it through the far field intensity patterns in Fig. 4. As $|\delta|$ increases, the isotropic emission of mode pair when $|\delta| = 0$ turns into the bi-directional emission and the mode pairs in each step have the same tendency for the far-field intensity distribution regardless of parity. The bi-directionality is bestly improved at $|\delta| = 0.15$. Incidentally, if $|\delta| \geq 0.2$, the maximum value of refractive index profile requires a large rise above 4 which is difficult to implement, but the far field distribution still has bi-directionality.

B. Purity Factor for cWGMs

We are here to present another tool for characterizing cWGMs. In general, when the homogeneous circular cavity is progressively distorted by the shape deformation, WGMs with perfect rotational symmetry begin to lose their inherent properties, accompanied by the Q -spoiling and the pattern distortion by the synthesis of several angular momentum components. The angular momentum decomposition is very useful method for analyzing such the angular momentum distribution [22]. The spread of m derived from the analysis of angular momentum components for a resonant mode can be used to gauge how

much the resonance in a slightly deformed cavity is distorted from a specific resonance in the circular cavity. Such distortion also occurs at the resonances in TCs. In the case of homogeneous cavities, the distortion is due to the effect of shape deformation, whereas in the case of C-S circular TC without shape deformation, it is caused by the non-uniformity of the relative refractive index at the boundary interface. The variation of the distortion rate for each mode according to the change of the system parameters has different criteria according to the lifetime and wavelength of the resonance, but it is sufficient to check how long the WGM characteristics of the circular cavity are maintained in the cWGM.

To analyze the inherent mode properties inside TCs, we introduce the angular momentum distribution in RV space equivalent with TP space. In RV space, the wave function inside the circular cavity can be expanded to cylindrical harmonics in polar coordinates as follows:

$$\psi(r_{\text{RV}}, \phi_{\text{RV}}) = \sum_{m=-\infty}^{\infty} \alpha_m J_m(n_{\text{in}}^{\text{RV}} k_r r_{\text{RV}}) \exp(im\phi_{\text{RV}}),$$

where r_{RV} and ϕ_{RV} are the radius and angle of the position on the data pickup domain, respectively, $+$ ($-$) signs of angular momentum index mean CCW (CW) traveling-wave components, α_m is the angular momentum distribution for m , and J_m is the m th-order Bessel function of the first kind. α_m is obtained through the Fourier expansion of the above equation. Note that the data pickup domain must be chosen as a concentric circle with a center of mass in the RV space, taking into account the spatial transformation by conformal mapping. From the above angular momentum distribution, our newly proposed measurand

that estimates the mode distortion rate, namely purity factor, can be simply defined as follows :

$$P = \frac{|\alpha_d|^2}{\sum_{m=0}^{\infty} |\alpha_m|^2},$$

where α_d is that for a dominant angular momentum index d . Under the our situation of standing wave conditions by axis symmetry, we only need to take one component, CCW or CW. This P -factor means the contribution of resonance with $m = d$ in the circular cavity in forming a specific resonance we are going to observe in TCs.

To investigating the change of distortion rate for the cWGM, we obtained the above P -factor for M(13,1) in the range of $0 \leq |\delta| \leq 0.4$ where the data pickup domain $r_{RV} = 0.8$. We plotted it in Fig. 5 attaching the P -factor for M(13,2) for comparison. The $|\delta|$ -dependent increase in the heterogeneity of the relative refractive index at the boundary interface, which acts as an effective deformation effect, reduces overall the P -factor for both modes. Here, it should be noted that the variation of the P -factor for M(13,1) is relatively very small compared with M(13,2). It means that the resonance properties in the circular cavity are maintained fairly well in cWGMs with $l = 1$.

V. SUMMARY

In this paper, we have newly proposed a construction scheme for TC without the resizable parameter related to

TIR condition, and, in the C-S circular TC using it, investigated the characteristic changes of a cWGM of which isotropic emission breaks in bi-directional emission as the C-S parameter increases. The enhancement of distortion effect on the modes due to the pure spatial refractive index variation according to the C-S parameter can be verified through the newly defined purity factor P indicating how much the nature of WGM in the circular cavity is maintained via the angular momentum distribution in the RV space. In conclusion, it has been examined that the C-S circular TC can produce the bi-directional emitting cWGMs of which P -factor is nearly one.

ACKNOWLEDGMENTS

We would like to thank S.-J. Park, Y. Kim, and Y.-H. Lee for helpful discussions. This work was supported by the National Research Foundation of Korea (NRF) grant funded by the Korean government (MSIP) (2017R1A2B4012045 and 2017R1A4A1015565) and the Institute for Basic Science of Korea (IBS-R024-D1).

-
- [1] Y. Kim, S. H. Lee, J. W. Ryu, I. Kim, J. H. Han, H. S. Tae, M. Choi, and B. Min, "Designing whispering gallery modes via transformation optics," *Nature Photonics* **10**, 647 (2016).
 - [2] Chang, R. K., and A. J. Campillo, *Optical Processes in Microcavities* (World Scientific, Singapore, 1996).
 - [3] K. J. Vahala, "Optical microcavities," *Nature* **424**, 839 (2003).
 - [4] H. Cao and J. Wiersig, "Dielectric microcavities: Model systems for wave chaos and non-Hermitian physics," *Rev. Mod. Phys.* **87**, 61 (2015).
 - [5] J. U. Nöckel and A. D. Stone, "Ray and wave chaos in asymmetric resonant optical cavities," *Nature* **385**, 45 (1997).
 - [6] S.-B. Lee, J.-H. Lee, J.-S. Chang, H.-J. Moon, S. W. Kim, and K. An, "Observation of Scarred Modes in Asymmetrically Deformed Microcylinder Lasers," *Phys. Rev. Lett.* **88**, 033903 (2002).
 - [7] S. Shinohara, T. Harayama, T. Fukushima, M. Hentschel, T. Sasaki, and E. E. Narimanov, "Chaos-Assisted Directional Light Emission from Microcavity Lasers," *Phys. Rev. Lett.* **104**, 163902 (2010).
 - [8] S. Sunada, S. Shinohara, T. Fukushima, and T. Harayama, "Signature of Wave Chaos in Spectral Characteristics of Microcavity Lasers," *Phys. Rev. Lett.* **116**, 203903 (2016).
 - [9] W. D. Heiss, "Repulsion of resonance states and exceptional points," *Phys. Rev. E* **61**, 929 (2000).
 - [10] J. Wiersig, "Formation of Long-Lived, Scarlike Modes near Avoided Resonance Crossings in Optical Microcavities," *Phys. Rev. Lett.* **97**, 253901 (2006).
 - [11] J. Wiersig and M. Hentschel, "Unidirectional light emission from high-Q modes in optical microcavities," *Phys. Rev. A* **73**, 031802(R) (2006).
 - [12] S.-Y. Lee, J.-W. Ryu, J.-B. Shim, S.-B. Lee, S. W. Kim, and K. An, "Divergent Petermann factor of interacting resonances in a stadium-shaped microcavity," *Phys. Rev. A* **78**, 015805 (2008).
 - [13] J. Wiersig, S. W. Kim, and M. Hentschel, "Asymmetric scattering and nonorthogonal mode patterns in optical microspirals," *Phys. Rev. A* **78**, 053809 (2008).
 - [14] J.-W. Ryu, S.-Y. Lee, and S. W. Kim, "Coupled non-identical microdisks: Avoided crossing of energy levels and unidirectional far-field emission," *Phys. Rev. A* **79**, 053858 (2009).
 - [15] C.-W. Yi, J. Kullig, and J. Wiersig, "Pair of Exceptional Points in a Microdisk Cavity under an Extremely Weak Deformation," *Phys. Rev. Lett.* **120**, 093902 (2018).

- [16] S.-J. Park, I. Kim, J. Cho, Y. Kim, and M. Choi, "Designing arbitrary-shaped whispering-gallery cavities based on transformation optics," *Opt. Express* **27**, 16320-16328 (2019).
- [17] I. Kim, J. Cho, Y. Kim, B. Min, J.-W. Ryu, S. Rim, and M. Choi, "Husimi functions at gradient index cavities designed by conformal transformation optics," *Opt. Express* **26**, 6851-6859 (2018).
- [18] M. Hentschel and H. Schomerus, "Fresnel laws at curved dielectric interfaces of microresonators," *Phys. Rev. E* **65**, 045603(R) (2002).
- [19] H. Schomerus and M. Hentschel, "Correcting Ray Optics at Curved Dielectric Microresonator Interfaces: Phase-Space Unification of Fresnel Filtering and the Goos-Hänchen Shift," *Phys Rev Lett.* **96**, 243903 (2006).
- [20] J. Unterhinninghofen, J. Wiersig, and M. Hentschel, "Goos-Hänchen shift and localization of optical modes in deformed microcavities," *Phys. Rev. E* **78**, 016201 (2008).
- [21] J.-W. Ryu, J. Cho, I. Kim, and M. Choi, "Optimization of conformal whispering gallery modes in limaçon-shaped transformation cavities," *Scientific Reports* **9**, 8506 (2019).
- [22] J. Wiersig, S. W. Kim, and M. Hentschel, "Asymmetric scattering and nonorthogonal mode patterns in optical microspirals," *Phys. Rev. A* **78**, 053809 (2008).